Supporting Information

Ferric ion substitution renders cadmium metal-organic framework derivatives for modulated Li storage based on local oxidation active center

Wei Jiang[a,d], Baihui Gao[a], Guosong Yan[a], Shichong Xu[c], Xianyu Chu[a], Guangbo Che[a,e], Bo Liu[a,*], Ming Lu[b,c,*], Chunbo Liu[a,d,*]

[a] *Key Laboratory of Preparation and Application of Environmental Friendly Materials (Jilin Normal University), Ministry of Education, Changchun 130103, PR China*

[b] *Shenyang National Laboratory for Materials Science, Institute of Metal Research, Chinese Academy of Sciences, Shenyang 110016, Liaoning, PR China*

[c] *Key Laboratory of Functional Materials Physics and Chemistry of the Ministry of Education, the Joint Laboratory of MXene Materials, Jilin Normal University, Changchun 130103, Jilin, PR China*

[d] *College of Engineering, Jilin Normal University, Siping, 136000, PR China*

[e] *College of Chemistry, Baicheng Normal University, Baicheng, 137000, P. R. China.*

***Corresponding authors.**

E-mail addresses:

luming@jlnu.edu.cn (M. Lu), liubo1999@jlnu.edu.cn (B. Liu), chunboliu@jlnu.edu.cn (C. Liu)

1. Figures and Tables

1.1. Crystal data

Crystal data was collected Bruker Smart Apex II CCD diffractometer with graphitemonochromatic Mo*Kα* radiation (λ = 0.71073 Å) at room temperature. The structures were solved by direct methods of *SHELXS-2014* and refined on F^2 by full-matrix least-squares using the *SHELXL-2014 within WINGX*. All the calculations were performed under *WINGX* program. All non-hydrogen atoms were refined anisotropically, and the hydrogen atoms of organic ligands and water molecules were generated geometrically. The crystallographic data for **Cd-MOF** is listed in Table S1, selected bond lengths and bond angles are summarized in Table S2.

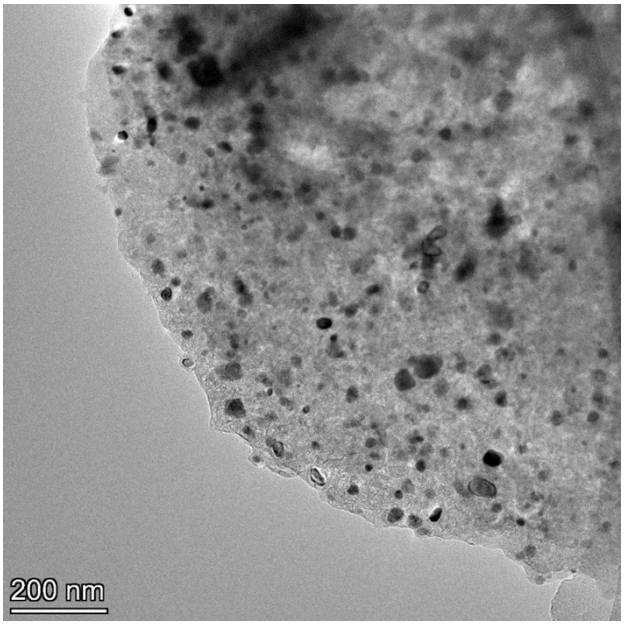

Fig. S1. TEM images of **Fe@Cd-MOFD**.

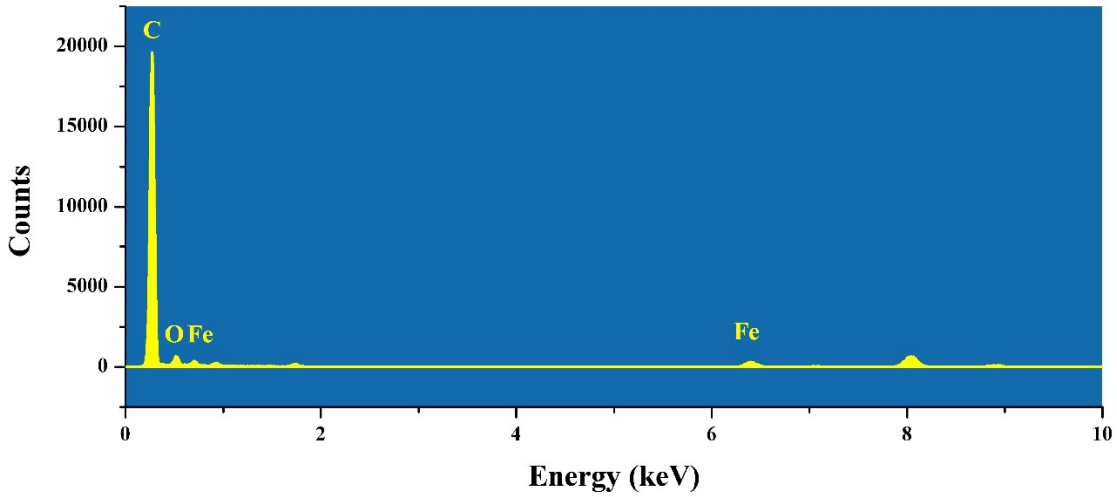

Fig. S2. EDX of **Fe@Cd-MOFD** obtained from TEM.

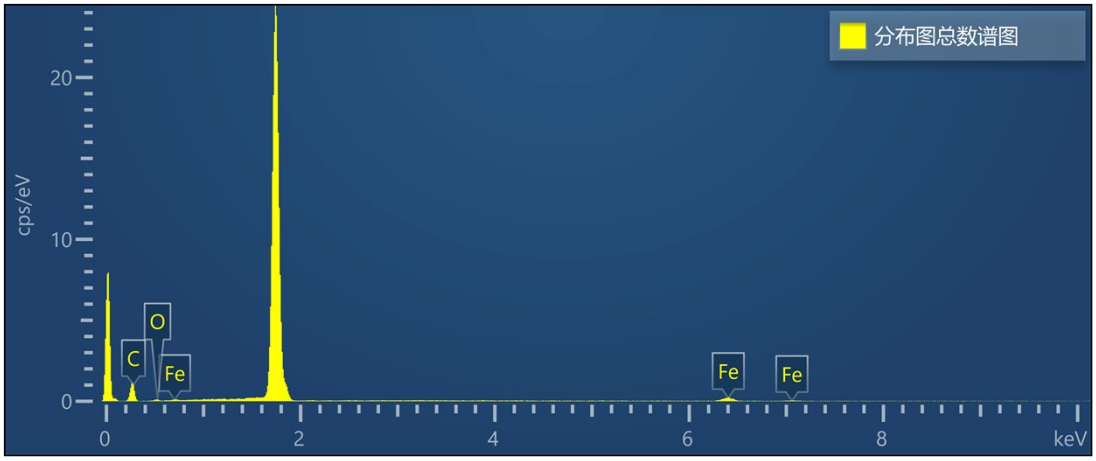

Fig. S3. EDX of **Fe@Cd-MOFD** obtained from SEM.

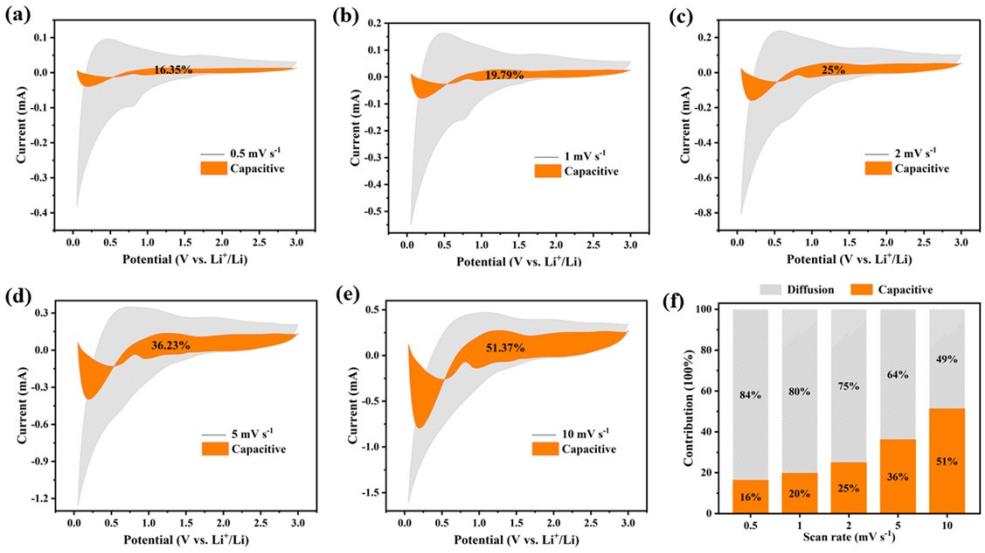

Fig. S4 (a-e) Capacitive contribution of the **Fe@Cd-MOFD** from the scan rate of 0.5-10 mV s^{-1}. (f) Contribution ratio of capacitive and diffusion at different scan rates.

To fully investigate the excellent performances of **Fe@Cd-MOFD** hollow nanostructures in LIBs, the reaction kinetics were analyzed by CV measurements at different scan rates from 0.5 to 10 mV s^{-1} (Fig. S4). According to previous reports, there is a power law between measured current and scan rate.

$$i = k_1 v + k_2 v^{1/2} \quad (1)$$

Where k_1 and k_2 are the constants at a fixed potential, v is the scan rate. The determination of k_1 and k_2 allows calculating the proportion of capacitive contribution ($k_1 v$) or diffused behavior ($k_2 v^{1/2}$). Fig. S4 shows that the capacitive contribution

gradually increased from 16.35 to 51.37% with the scan rate increasing from 0.5-10 mV s^{-1}.

Table S1 Selected crystallographic data for **Cd-MOF**.

Compound	**Cd-MOF**
Formula	$C_{47}H_{52}CdN_3O_{16}$
Mr	1027.34
Crystal system	Monoclinic
Space group	$P2_1/n$
a (Å)	21.479(4)
b (Å)	7.9353(16)
c (Å)	32.660(6)
α (°)	90
β (°)	105.015(4)
γ (°)	90
V (Å^3)	5376.6(18)
Z	4
D_{calc} (g cm^{-3})	1.215
F(000)	1984
R_{int}	0.0932
GOF on F^2	1.012
$R_1{}^a$ [I>2σ(I)]	0.0907
$wR_2{}^b$ (all data)	0.3211
CCDC	2151098

$^aR_1 = \Sigma||F_o| - |F_c||/\Sigma|F_o|$. $^bwR_2 = \{\Sigma[w(F_o^2-F_c^2)^2]/\Sigma w(F_o^2)^2]\}^{1/2}$.

Table S2 Selected bond distances (Å) and angles (°) for **Cd-MOF.**

Bond	Distance	Bond	Distance
Cd(1)-O(1)	2.3663(39)	Cd(1)-O(7)	2.2692(37)
Cd(1)-O(2)	2.4955(37)	Cd(1)-O(8)	2.5051(41)

Cd(1)-O(3)	2.2521(55)	Cd(1)-O(13)	2.3045(40)
Cd(1)-O(4)	2.4991(24)		
Angle	(°)	Angle	(°)
$O(3)^{\#1}$-Cd(1)-$O(7)^{\#2}$	136.0(3)	$O(3)^{\#1}$-Cd(1)-$O(7)^{\#2}$	136.0(3)
$O(3)^{\#1}$-Cd(1)-O(13)	109.4(3)	$O(3)^{\#1}$-Cd(1)-O(13)	109.4(3)
$O(7)^{\#2}$-Cd(1)-O(13)	87.5(3)	$O(7)^{\#2}$-Cd(1)-O(13)	87.5(3)
$O(3)^{\#1}$-Cd(1)-O(1)	133.4(3)	$O(3)^{\#1}$-Cd(1)-O(1)	133.4(3)
$O(7)^{\#2}$-Cd(1)-O(1)	87.8(3)	$O(7)^{\#2}$-Cd(1)-O(1)	87.8(3)
O(13)-Cd(1)-O(1)	82.5(3)	O(13)-Cd(1)-O(1)	82.5(3)
$O(3)^{\#1}$-Cd(1)-O(2)	83.7(3)	$O(3)^{\#1}$-Cd(1)-O(2)	83.7(3)
$O(7)^{\#2}$-Cd(1)-O(2)	123.5(3)	$O(7)^{\#2}$-Cd(1)-O(2)	123.5(3)
O(13)-Cd(1)-O(2)	119.8(3)	O(13)-Cd(1)-O(2)	119.8(3)
O(1)-Cd(1)-O(2)	53.2(2)	O(1)-Cd(1)-O(2)	53.2(2)
$O(3)^{\#1}$-Cd(1)-$O(8)^{\#2}$	101.7(3)	$O(3)^{\#1}$-Cd(1)-$O(8)^{\#2}$	101.7(3)

Symmetry transformations used to generate equivalent atoms: $^{\#1}$ -*x*+1, -*y*-1, -*z* $^{\#2}$ -*x*+1/2, *y*-1/2, -*z*+1/2 CCDC number：2151098

Table S3 The EDS data of **Fe@Cd-MOFD**.

	wt%	at%
C	70.39	85.72
O	10.01	9.15
Fe	19.60	5.13